Available online at www.sciencedirect.com

ScienceDirect

Energy Procedia 45 (2014) 502 – 511

Energy Procedia

68th Conference of the Italian Thermal Machines Engineering Association, ATI2013

Analysis of flat plate honeycomb seals aerodynamic losses: effects of clearance

Daniele Massini[a], Bruno Facchini[a], Mirko Micio[b], Cosimo Bianchini[b], Alberto Ceccherini[c], Luca Innocenti[c]

[a]*Industrial Engineering Department, University of Florence, Via S.Marta 3, Florence 50139, Italy*
[b]*ERGON Research s.r.l., Via Panciatichi 92, Florence 50127, Italy*
[c]*GE Oil & Gas, Via F.Matteucci 2, Florence 50127, Italy*

Abstract

Among the various type of seals used in gas turbine secondary air system to guarantee sufficient confinement of the main gas path, honeycomb seals well perform in terms of enhanced stability and reduced leakage flow. Reliable estimates of the sealing performance of honeycomb packs employed in industrial gas and steam turbines, are however missing in literature, thus, in order to evaluate the complete characteristic curve of the seals in the wide range of working conditions, an experimental campaign was planned. This work reports the findings of an experimental campaign aimed at evaluating aerodynamic losses within honeycomb seals.

Due to the generally large amount of honeycomb cells typically present in real seals, it would be convenient to treat the sealing effect of the honeycomb pack as an increased distributed friction factor on the plain top surface that is why the simplest configuration, the honeycomb facing a flat plate, is employed in this paper. The geometry of the hexagonal cell and the investigated clearances were chosen to well represent actual honeycomb packs employed in industrial compressors. First the pressure distribution within the seal was analysed verifying that downstream the first 5 rows of cells, where entrance effects are predominant, the relative pressure drop is almost constant thus the use of an equivalent friction factor is appropriate to characterize the seal. Subsequent analysis focused on the characterization of the friction factor as function of the Reynolds number with the aim of establishing the proper geometrical scaling to achieve flow conditions similar to real turbine most critical ones.

The different behaviour of the honeycomb sealing depending on the hexagonal cell arrangement and dimensions was evaluated in terms of friction factor.

Comparison with results coming from a previous CFD investigation is also presented and discussed in this paper.

Selection and peer-review under responsibility of ATI NAZIONALE

Keywords: honeycomb, sealing, friction factor, centrifugal compressors, secondary air system

* Daniele Massini. Tel.: +39-055-4796439.
E-mail address: daniele.massini@htc.de.unifi.it

Selection and peer-review under responsibility of ATI NAZIONALE
doi:10.1016/j.egypro.2014.01.054

1. Introduction

Centrifugal compressors rotor-dynamic stability can be affected by reaction forces generated in correspondence of seals, which are determined by geometrical and working parameters challenging to reliably take into account effects due to the very narrow clearances, high pressure and high relative speed rotor motion [1]. On the other hand reducing leakages, enhancing working pressures and rotational speeds are fundamental to reach high sealing efficiency.

Different kinds of seals may be employed in the seal's gaps to confine the main flow path, among which honeycomb seals perform well also in terms of rotor-dynamic stability. Derived from aircraft engine technology they are composed by a honeycomb surface stator running against a rotor, which can be smooth or equipped with other type of seal, such as labyrinth, stepped or a second honeycomb pack, a scheme is illustrated in figure 1.

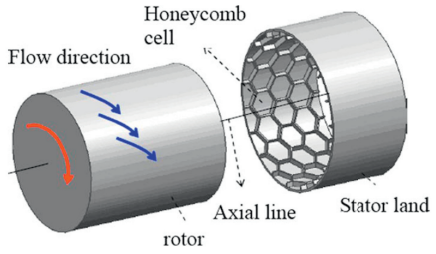

Fig. 1. Honeycomb annular seal

In the late 1980s Childs et al. [2] published the first research on honeycomb seals, analysing leakage mass flow reduction and the enhanced rotor-dynamic stability. After a wide experimental investigation, in which seven types of honeycomb stator seals were analysed, results showed that honeycomb seals were better, in terms of rotor-dynamic stability, than labyrinth seals if a swirl brake is not present.

A comparison between experimental and theoretical predictions was performed, on this honeycomb seal configuration, by Childs and Kleynhans [3]. They found six parameters influencing rotor dynamics coefficients: pressure ratio across the seal, seal inlet pressure, rotor speed, seal inlet fluid rotation, seal clearance and honeycomb cell width.

In 2000, Al-Qutub et al. [4], performed an experimental analysis on a static test rig. They found out a dependency of friction factor on Reynolds number and clearance only. Entrance loss coefficient evaluation was performed both in smooth and honeycomb case, showing no effect of the inlet Mach number, seal clearance and Reynolds number: it was found to be 50% higher for honeycomb seals than for smooth.

In 2001, He et al. [5], performed an experimental investigation on a rotating test rig with three different honeycomb seals, varying cell sizes, and a labyrinth seal. Cell size and seal clearance were found to be important parameter, with rotor rotational speed, having great influence on leakage mass flow: in particular a leakage reduction was found with rotor speed increase.

Three different friction factor models were compared by Childs and D'Souza [6], using the two-control-volume bulk flow model developed by Childs and Ha [7] and Kleynhans [8]. The rotor-dynamic predictions given were coincident for every model, except for low frequency range (60 – 70[Hz]) where the different models brought to different effective-damping coefficients.

Chochua et al. [9] performed a steady state CFD simulation on a seal composed by two honeycomb flat plates experimentally studied by Ha and Childs. The results showed that flow structures developing inside the cells vary with Reynolds number. Simulations were not capable to predict the friction factor jump phenomenon observed in the experiments.

In 1996 Kleynhans [8] developed a 1D code based on a constant temperature bulk-flow model, in order to estimate the friction factor for rotor-dynamic calculations of gas annular honeycomb seals. Since 2004 Childs et al. [10], [11], [12] made a series of experiments on a rotating test rig in order to provide numerical validation for the 1D made by Kleynhans. The model seems to well predict the frequency response of the experiments, suggesting the use of a swirl brake at the inlet of the seal to rise its stability characteristics. In the last work the authors pointed out the importance on the measurements of friction factor coefficients with the goal of improving the stiffness coefficients prediction.

Recently Ertas et al. [13] performed an experimental analysis on three types of non-contact seals: labyrinth, honeycomb and fully partitioned damper seal. The goal of the analysis was to compare rotor-dynamic force coefficients for the typical seals used at the balance piston in gas centrifugal compressors. The results showed that first part of the seal is strongly influenced by pre-swirl, this effect decreases rapidly as the cavity number increases. The rotor speed has more importance in generating destabilizing forces at the center of the seal, which decreases towards the end.

Works found in literature underline the importance of friction factor coefficient evaluation for the prediction of the seals rotor-dynamic characteristics.

Present paper reports the validation and the first measurements on a new steady parallel plates test rig equipped for friction factor evaluation, in particular its evolution with Reynolds number.

The test rig configuration consists of a plate equipped with honeycomb cells facing on a smooth surface. Different parameters can be changed in order to point out their influence on friction factor coefficient: clearance, cell width, cell depth, cell orientation.

This work reports the measurements carried out on the smooth configuration and three other geometries. Comparison with numerical results coming from a previous CFD study aimed at guiding the test rig design [14] is also presented, focusing the considerations on the friction factor evolution found in the experimental investigation.

Nomenclature

A	Area [mm^2]
C	Cell width[mm]
D	Cell depth[mm]
D_e	Equivalent diameter[mm]
D_h	Hydraulic diameter[mm]
f_f	Friction factor[$-$]
H	Seal clearance[mm]
L	Seal length[mm]
$\dot{m}$	Mass flow rate[kg/s]
M_a	Mach number[$-$]
P	Static pressure[Pa]
Re	Reynolds number[$-$]
T	Cell thickness[mm]
V	Velocity[m/s]
W	Seal width[mm]
X	Span-wise direction[$-$]
Y	Normal direction[$-$]
Z	Stream-wise direction[$-$]
z	Stream-wise position[mm]

Greeks

ϵ	Roughness[$-$]
γ	Specific heat ratio[$-$]
μ	Dynamic viscosity[Pas]
ρ	Density[kg/m^3]
σ	Standard deviation[$-$]
τ_f	Shear stress due to wall friction[Pa]

Subscripts

w	Wet
max	Maximum
min	Minimum

Acronyms

SF	Scale Factor

2. Experimental facility and procedure

2.1. Test rig

Measurement campaign was carried out at the Industrial Engineering Department in University of Florence, using a stationary test rig designed on purpose. Numerical campaign exploiting steady state RANS analysis was performed to help the design of the facility, results can be found in [14] and they will be compared in this paper with experimental measurements.

The facility consists in an open loop suction type wind tunnel connected with the laboratory vacuum system composed of two vacuum pumps with a capacity of 900$[m^3/h]$ each and two with 300$[m^3/h]$ each. A scheme is shown in figure 2.

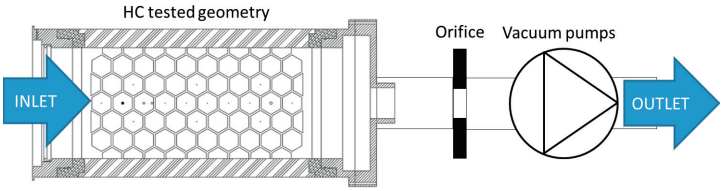

Fig. 2. Test rig layout

The geometry investigated reproduces, without rotational effects, the sealing system of the type "honeycomb on smooth" and is scaled up with a scale factor $SF = 30$, in order to have more confidence and accuracy on clearance dimensions.

The maximum mass flow rate and Reynolds number reached in every test depends on the pressure drop across the test article: in the worst configuration $\dot{m}_{max} = 0.3[kg/s]$, $Re_{max} = 90000$ for $\Delta P = 30000[Pa]$, in the best $\dot{m}_{max} = 0.430[kg/s]$, $Re_{max} = 130000$, for $\Delta P = 600[Pa]$.

Pressure scanners Scanivalve DSA 3217, with temperature compensated piezoresistive relative pressure sensors, with 16 channels are used for pressure measurements: the variability of the pressure drop in different tests imposes the use of pressure scanners with different scales in order to reach the best accuracy: 5PSI(34500$[Pa]$) DSA with 17.223$[Pa]$ accuracy and 1PSI (6900$[Pa]$) DSA with 6.9$[Pa]$ accuracy.

T-type thermocouples are used for temperature measurements with uncertainty of $\pm 0.5[^\circ C]$; Agilent 34970A is used for the thermocouple acquisition. A thermocouple is disposed in correspondence of the inlet in order to measure the flow total temperature.

Test rig is equipped with pressure taps in both sides, disposed in two rows along the Z direction, facing each other. They are spaced differently in the two plates because on honeycomb side they are placed in the center of the cells: the distance between them vary. They are used to measure the friction factor coefficient along the test article.

Further pressure taps, out of the principal row, are present in the smooth side to provide information on the homogeneity of the flow in span direction: considering Geo2 (see tab1) one row faces the center of the cells, the other the cells' wall (figure 3).

Fig. 3. Pressure taps position on smooth plate

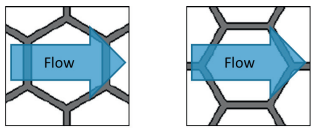

Fig. 4. Cell orientation configuration

The pressure drop and the temperature of the air flowing through a calibrated orifice in the pumps circuit allows to know the air mass flow.

Both the honeycomb and smooth plates are made of plexiglass in order to minimize heat conduction. Total temperature can be considered constant in the test rig. For this reason knowing total inlet temperature, static pressure

and the air mass flow rate is possible to completely characterize every parameter used to compute the friction factor coefficient in every measuring point as explained below.

The friction factor distribution is the basis of this study; the formula used for its computation derives from the Fanno model: considering air as an ideal gas, with constant specific heat, steady, adiabatic, neglecting effects of area change, body forces and work crossing the control surface.

We can assume one dimensional flow thanks to the high aspect ratio W/H and for the same reason the hydraulic diameter $D_h = 2H$. The momentum equation along the Z direction is hence: $\tau_f A_w - AdP = \rho AVdV$.

Defining the Fanning friction factor as $f_f = (\tau_f/(0.5\rho V^2)$ and substituting in previous equation we reach:

$$-dP - 2\rho V^2 f_f \frac{dz}{D_h} = \rho V dV \tag{1}$$

This last equation can be modified as:

$$f_f = \frac{D_h}{2}\frac{1}{M}\left(\frac{1-M^2}{(1+\frac{\gamma-1}{2}M^2)\gamma M^2}\right)\frac{dM}{dz} \tag{2}$$

The Reynolds number is calculated in the following using the hydraulic diameter $Re = \rho V D_h/\mu$.

The measure was done in steady conditions, three independent acquisitions for every measuring point were averaged to obtain mean value.

2.2. Honeycomb geometry: test matrix

The analysed geometry is usually employed at the balance drum in centrifugal compressors, with the goal of limiting the leakage flow in those points where big pressure gradients are present.

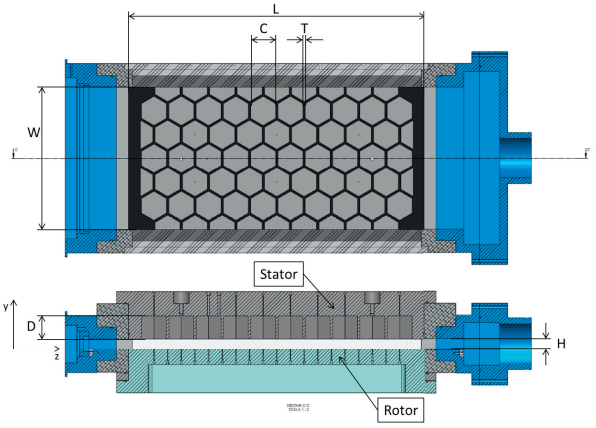

Fig. 5. Honeycomb seal geometry

The effectiveness of the honeycomb seals is related to the cells geometry, figure 5 and orientation, figure 4; that is fully defined by cell width C, cell depth D, cell thickness T, clearance H and orientation: facing edge or facing vertex.

Every test was performed varying the Reynolds number in a range between 40000 and the maximum allowed by the geometry and clearance.

Before starting honeycomb tests, test rig validation was performed on a “smooth vs smooth” test providing results comparable with theory and correlations, the validation will be discussed below in section 3.2.1.

Three different geometries were tested each with three different clearances: their characteristics, scaled on the test section minimum clearance H_{min}, are summarized in table 1.

Table 1. Cells geometry

Geometry	Cell Width(C/H_{min})	Cell Depth(D/H_{min})	Cell Thickness(T/H_{min})	Section width(W/H_{min})	Cell Orientation	Clearance(H/H_{min})
Smooth	\	\	\		\	
Geo1	10.24	13.66	0.97	58.3	Vertex	1; 2.46; 4.41
Geo2	10.24	9.43	0.97		Edge	
Geo3	7.8	12.68	0.4		Edge	

3. Experimental results

3.1. Uncertainty analysis

The uncertainty analysis was performed following the standard ANSI/ASME PTC 19.1 [15] based on the Kline and McClintock method [16].

Given that friction factor is an indirect measurement the uncertainty of the measurement was computed using the general error propagation formula: $\sigma_g = \sqrt{\left(\frac{\partial g}{\partial x}\right)^2 \sigma_x^2 + \left(\frac{\partial g}{\partial y}\right)^2 \sigma_y^2 + \left(\frac{\partial g}{\partial z}\right)^2 \sigma_z^2}$

Where $g = g(x, y, z)$ is the computed value, x, y, z the variables influencing the calculation and σ is the uncertainty.

Instruments uncertainties, given by the data-sheets, are constant values: 0.05% and 0.1% of full range for DSA5PSI and DSA1PSI respectively; 0.5[K] for thermocouples.

The error on Reynolds number was computed to be under 5%.

Given that the friction factor computation is based on the pressure drop measurement, which increases with the losses due to clearance reduction or velocity increase, the instrument uncertainty has a decreasing importance and so the total one.

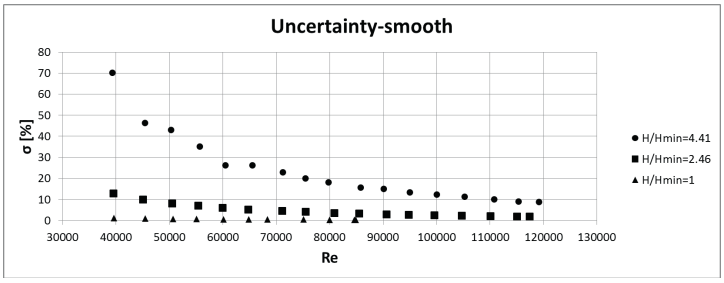

Fig. 6. Friction factor uncertainty for different clearances in validation tests (smooth surfaces)

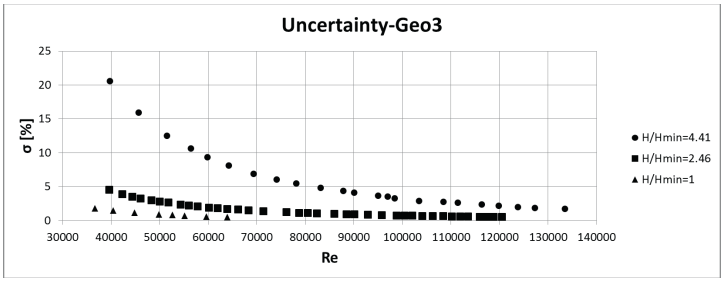

Fig. 7. Friction factor uncertainty for different clearances in a test article measurements: it is well representative of all geometries

Figures 6 and 7 show uncertainties in validation tests ("smooth vs smooth" case) and Geo3 tests ("honeycomb vs smooth" case). They underline three different trends:

- all the curves have a decreasing trend with Reynolds number: this is due to the increase of the pressure losses with velocity;
- clearance reduction causes pressure losses increase, the effect is a shift of the curves towards lower values;

- the uncertainty values in figure 6 are higher than those in firgure 7: this is due to the presence of the honeycomb surface in the second case.

Unfortunately in the largest clearance configuration the uncertainty is very high, both in "smooth vs smooth" and "honeycomb vs smooth"; in the intermediate, error is under the 15% and 5% respectively. In the smallest clearance, error is under the 2% for geometry case, and under the 1% in the smooth case.

3.2. Test rig validation

Before starting the measurement campaign the test rig was validated: leak test, repeatability of the tests, homogeneity of the flow, and accordance with the theory of friction factor in smooth rectangular ducts was checked.

After every assembling of the model a test was performed in order to check the entity of the leak through the sealing: the inlet was closed and the vacuum pumps switched on until the pressure inside the facility was 40[kPa], then the time that the pressure took to reach ambient condition was measured and the leakage mass flow rate computed by equation 3:

$$\dot{m}_{loss} = \frac{dP}{dt}\frac{V}{RT} \tag{3}$$

The leakage was always less than 2% of the minimum mass flow rate measured in tests.

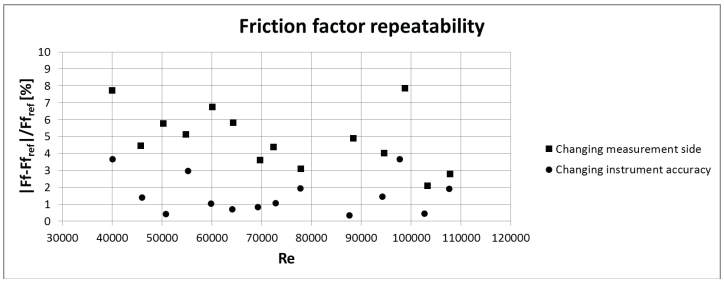

Fig. 8. Friction factor repeatability from test on Geo2 $H/H_{min} = 4.41$

Every test was repeated twice or more, measuring both on smooth and honeycomb side or using instruments with different accuracy (17.223[Pa] instead of 3.45[Pa]). The results obtained are consistent: the double check is shown in figure 8 where the differences between the curves are plotted; the maximum difference is under the 10%.

The homogeneity of the flow was checked using two different rows of pressure taps in the measurement and comparing the results.

Numerical investigation results presented in [14] show the presence of a possible preferential way for air flow in facing edge configuration and the need of fewer rows of cells for the friction factor to stabilize.

Pressure measurements on different span positions were performed to check this possibility and the flow was found to be perfectly homogeneous. The friction factor distribution was found to be not influenced by inlet effects.

3.2.1. Smooth rectangular ducts

Friction factor has been studied deeply in the past and numerous correlations exist to help engineers to solve design problems, unfortunately they usually refer to circular ducts and it is necessary to find parameters to link those results to ducts having rectangular section.

We used two parameters: the hydraulic diameter D_h and the equivalent diameter $D_e = 1.30 \cdot (ab)^{0.625}/(a+b)^{0.250}$ (a and b are the rectangular dimensions), defined as the diameter of the circular duct in which the flow has the same mass flow rate and pressure drop [17].

Both the definitions have been used to solve the most famous correlation to compute the Darcy friction factor, the Colebrook-White formula [17]:

$$\frac{1}{\sqrt{f_f}} = -2\log\left\{\frac{\epsilon}{3.7D_h} + \frac{2.51}{Re_{D_h}\sqrt{f_f}}\right\} \tag{4}$$

Where Re_{D_h} is the Reynolds number computed using the duct hydraulic diameter D_h.

Tests with "smooth vs smooth" configuration have been performed for every clearance, and results compared with the friction factor obtained from eq. 4.

In figure 9 the relative difference between the friction factor coefficients measured for every clearance and the ones computed using Colebrook equation is plotted: as it is possible to see the maximum distance is in correspondence of the maximum clearance and is under 15%, the other two cases are under 6%. It is important to underline the fact that the measure done with maximum clearance has the worst accuracy of the whole campaign considering the small pressure drop, moreover the Colebrook correlation is considered accurate within the 15%.

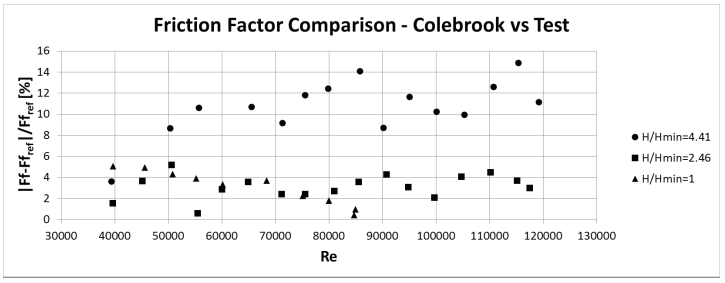

Fig. 9. Comparison Friction factor-Colebrook vs test

Another method used to validate the experimental results is focused on the equivalent diameter D_e: it is possible, knowing the geometry of the duct and the mass flow rate of every test, to calculate the friction factor for the equivalent circular duct and use it to estimate the pressure drop. It is possible then to compare the pressures calculated with the ones measured from taps as it has been done in figure 10.

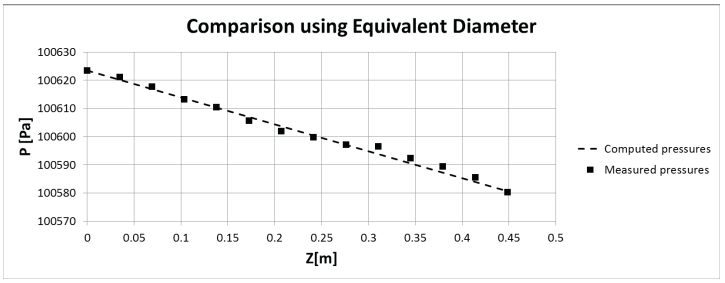

Fig. 10. Comparison: Pressure from theory and tests-Data from test smooth vs smooth $H/H_{min} = 4.41$

This kind of comparison has been done for every test, the relative difference between calculated and measured pressures is found to be always lower than 6%.

3.3. Results

Friction factor coefficients are shown with their evolution with Reynolds number and scaled on the smooth results for every clearance, in the form $FF = ff/ff_0$ where ff is the coefficient from honeycomb geometries and ff_0 from smooth cases.

In figure 11 results for the three different clearances are summarized for every geometry tested. It is possible to see the presence a good gain in comparison with smooth cases: the lower friction factor coefficient in honeycomb configuration is still three times higher than the one evaluated in smooth configuration.

A common characteristic can be underlined: friction factor coefficients do not have a monotonic trend with the clearance dimension as may be expected. The smallest friction factor values are in correspondence of the maximum clearance, friction factor is slightly higher for the minimum one, is then visible the highest friction factor for the intermediate clearance.

Measures performed by Ha et al. [18] confirm no monotonic effect with clearance and even a reverse trend changing other geometrical parameter, as cell width.

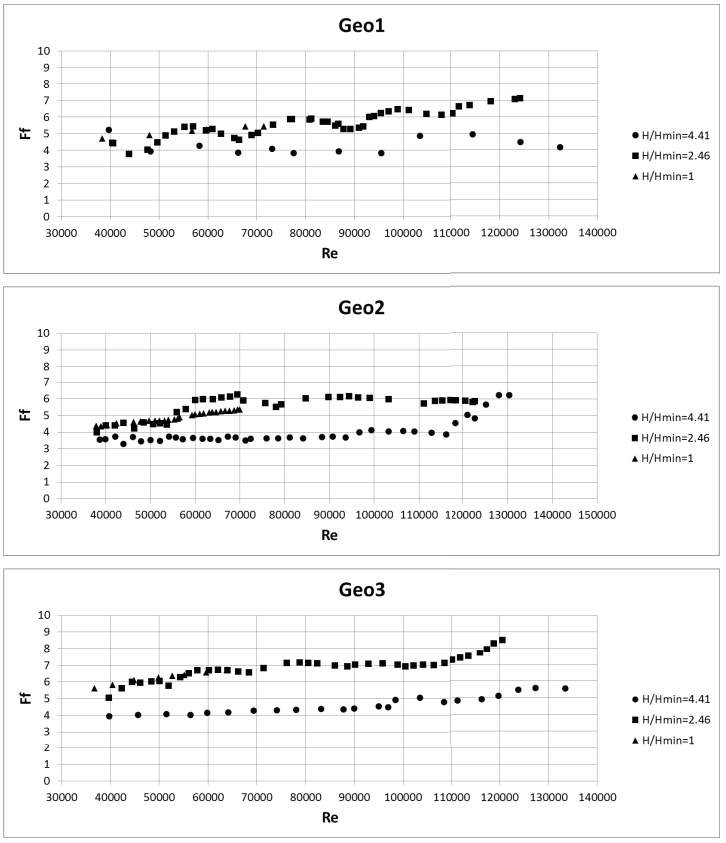

Fig. 11. Friction factor coefficients for Geo1, Geo2, Geo3-All clearances

The greatest effect seen is related to cell width reduction which causes a shift of the friction factor coefficients towards a higher level: this is due to the fact that the flow has to overcome more cells.

The friction factor evolution with Reynolds for the intermediate clearance does not have a definite trend but it is full of peaks and valleys. The number, magnitude and the Reynolds of these peaks and valleys changes with the geometry: Geo1 has the minimum number with the maximum intensity, while Geo3 has the minimum intensity.

During tests the presence of whistles coming from the test rig was noted: they seemed to have a maximum or a minimum in correspondence of the friction factor peaks and valleys.

It is known the fact that flow-acoustic interaction affects friction factor coefficients evaluated in honeycomb seals, this is due to the fact that the flow enters in the cavities generating vortices that interact with the main flow. That acoustic phenomena present in the facility can have an effect also on the time averaged pressure losses.

Ha et al. in [19] tried to explain the presence of friction factor jumps at difference Reynolds numbers by the acoustic theory and proposed the use of the Strouhal number as the correct parameter to show the friction factor evolution.

This kind of study can be taken into account in our future measurement campaigns.

4. Conclusions and future work

Experimental investigation on friction factor of flat plate honeycomb seals was performed. The measurement campaign consisted in a careful test rig validation followed by the analysis of three different geometry configurations.

All the measurements were conducted varying the Reynolds number between 30000 and 130000, three different clearance configurations were tested for every geometry.

Measurements were compared with results from a previous numerical campaign [14]: homogeneity of the flow was checked in stream and span direction and no influence due to cell orientation was verified.

The test rig validation, in "smooth vs smooth" configuration, gave results in accordance with literature. A double check was performed:

- friction factor coefficients measured were directly compared with the ones computed from Colebrook-White formula 4 calculated with the hydraulic diameter;
- starting from facility geometry and mass flow rate, pressure drop inside the test rig was computed, using Colebrook-White formula calculated with the equivalent diameter, and compared with measured pressures.

Both the checks gave good results confirming the test rig was well designed and the measurements well performed.

The friction factor results on honeycomb geometries are far from what could be expected: there is no monotonic trend with clearance neither with Reynolds number.

The intermediate clearance presented a weird behaviour, presenting peaks and valleys in the Reynolds evolution, for all the geometries: the whistles generation heard during tests makes to think about a flow-acoustic interaction. This phenomenon has to be understood and more tests will be performed using microphones and hot wire anemometer.

More geometries will be tested in order to decouple every geometric variable influencing the friction factor behaviour.

References

[1] Childs, D.W., Vance, J.M.. Annular gas seals and rotordynamics of compressors and turbines. Proceedings of the 26^{th} Turbomachinery Symposium, Turbomachinery Laboratory, Texas A & M University, September 14-16, ASME, New York 1997;:201–220.

[2] Childs, D.W., Elrod, D., Hale, K.. Annular honeycomb seals: Test results for leakage and rotordynamic coefficients; comparisons to labyrinth and smooth configurations. ASME J Tribol 1989;111:293–300.

[3] Childs, D.W., Kleynhans, G.F.. Experimental rotordynamic and leakage results for short (l/d = 1/6) honeycomb and smooth annular pressure seals. IMechE Proceedings, Fifth International Conference on Vibrations in Rotating Machinery, September 7-10, Bath, England 1992;111.

[4] Al-Qutub, A.M., Elrod, D., Coleman, H.W.. A new friction factor model and entrance loss coefficient for honeycomb annular gas seals. ASME J Tribol 2000;122:622–627.

[5] He, L., Yuan, X., Jin, Y., Zhu, Z.. Experimental investigation of the sealing performance of honeycomb seals. Chinese Journal of Aeronautics 2001;14(1).

[6] Childs, D.W., D'Souza, R.J.. A comparison of rotordynamic-coefficient predictions for annular honeycomb gas seals using three different friction-factor models. ASME J Tribol 2002;124:524–529.

[7] Childs, D.W., Ha, T.W.. Annular honeycomb-stator turbulent gas seal analysis using new friction-factor model based on flat plate tests. ASME J Tribol 1994;116:352–360.

[8] Kleynhans, G.F.. A two-control-volume bulk-flow rotordynamic analysis for smooth-rotor/honeycomb-stator gas annular seals. 1996.

[9] Chochua, G., Shyy, W., Moore, J.. Computational modeling for honeycomb-stator gas annular seal. Int J Heat Mass Transfer 2002;45:1849–1863.

[10] Childs, D.W., Wade, J.. Rotordynamic-coefficient and leakage characteristics for hole-pattern-stator annular gas seals-measurements versus predictions. ASME J Tribol 2004;126:326–333.

[11] Childs, D.W., Smalley, A.J., Camatti, M., Hollingsworth, J.R., Vannini, G., Carter, J.J.. Dynamic characteristics of the diverging taper honeycomb-stator seal. J TURBOMACH 2006;128:717–724.

[12] Childs, D.W., Sprowl, T.B.. A study of the effects of inlet preswirl on the dynamic coefficients of a straight-bore honeycomb gas damper seal. ASME J Eng Gas Turbines Power 2007;129:220–229.

[13] Ertas, B.H., Delgado, A., Vannini, G.. Rotordynamic force coefficients for three types of annular gas seals with inlet preswirl and high differential pressure ratio. ASME J Eng Gas Turbines Power 2012;134(042503):1–12.

[14] Bianchini, C., Micio, M., Maiuolo, F., Facchini, B.. Numerical investigation to support the design of a flat plate honeycomb seal test rig. ASME Turbo Expo 2013;(GT2013-95612).

[15] ASME, . Measurement uncertainty in instrument and apparatus. vol ANSI/ASME PTC 191-1985 of Performance Test Code, ASME 1985;(19).

[16] Kline, S.J., McClintock, F.A.. Describing uncertainties in single sample experiments. 1953.

[17] ASHRAE, . Duct Design. 2005.

[18] Childs, D.W., Ha, T.W.. Friction factor data for flat-plate tests of smooth and honeycomb surfaces. ASME J Tribol 1992;114:722–730.

[19] Keith, G.M., Ha, T.W., Bhattacharjee, P., Childs, D.W., Nielsen, K.K., Platt, J.P.. Friction factor jump in honeycomb seals explained by flow-acoustic interactions. ASME Turbo Expo: Power of land, Sea and Air 2009;(GT2009-60337):1–8.